

AD-A095 100

ARIZONA UNIV. TUCSON OPTICAL SCIENCES CENTER
SPECTRAL ANALYSIS STUDIES, (U)
JUL 79 W L WOLFE

F/6 17/5

F04701-77-C-0059

ML

UNCLASSIFIED

SD-TR-80-73

1 of 1
AD-A095 100
[Redacted]

END
DATE FILMED
3-81
DTIC

AD A095100

SD-TR-80-73

2

LEVEL 1

SPECTRAL ANALYSIS STUDIES

William L. Wolfe
Optical Sciences Center
University of Arizona
Tucson, Arizona 85721



July 1979

Final Report

Approved for public release;
distribution unlimited.

Prepared for

HQ SAMSO/DSY
P.O. Box 92960
Worldway Postal Center
Los Angeles, California 90009

REF ID: A6425

81 2 17 112

This final report was submitted by the Optical Sciences Center, University of Arizona, Tucson, Arizona 85721, under contract F04701-77-C-0059 with the USAF Hq Space Division, Los Angeles, CA 90009. This report has been reviewed and cleared for open publication and/or public release by the Public Affairs Office (PAS) in accordance with AFR 190-17 and DODD 5230.9. There is no objection to unlimited distribution of this report to the public at large, or by DTIC to the National Technical Information Service (NTIS).

This technical report has been reviewed and is approved for publication.

Dary M. Rowe

GARY M. ROWE, Capt
Project Engineer

James A. Janzen

JAMES A. JANZEN, Maj
Project Engineer

FOR THE COMMANDER

Richard B. Keel

RICHARD B. KEHL, Col
Director, Space Test Program
Deputy for Technology

UNCLASSIFIED

SECURITY CLASSIFICATION OF THIS PAGE (When Data Entered)

19 REPORT DOCUMENTATION PAGE		READ INSTRUCTIONS BEFORE COMPLETING FORM
1. REPORT NUMBER 18 SD-TR-80-73	2. GOVT ACCESSION NO. AD-A095 100	3. RECIPIENT'S CATALOG NUMBER
4. TITLE (and Subtitle) Spectral Analysis Studies,	5. TYPE OF REPORT & PERIOD COVERED Final	6. PERFORMING ORG. REPORT NUMBER
7. AUTHOR(s) William L. Wolfe	8. CONTRACT OR GRANT NUMBER(s) F04701-77-C-0059	9. PERFORMING ORGANIZATION NAME AND ADDRESS Optical Sciences Center University of Arizona Tucson, Arizona 85721
11. CONTROLLING OFFICE NAME AND ADDRESS HQ SAMSO/DYS P.O. Box 92960, Worldway Postal Center Los Angeles, California 90009	10. PROGRAM ELEMENT, PROJECT, TASK AREA & WORK UNIT NUMBERS 12 32	12. REPORT DATE Jul 1979
14. MONITORING AGENCY NAME & ADDRESS(if different from Controlling Office)	13. NUMBER OF PAGES 29	15. SECURITY CLASS. (of this report) Unclassified
16. DISTRIBUTION STATEMENT (of this Report) Approved for public release; distribution unlimited.	15a. DECLASSIFICATION/DOWNGRADING SCHEDULE	17. DISTRIBUTION STATEMENT (of the abstract entered in Block 20, if different from Report)
18. SUPPLEMENTARY NOTES	19. KEY WORDS (Continue on reverse side if necessary and identify by block number) Infrared Spectral analysis	
20. ABSTRACT (Continue on reverse side if necessary and identify by block number) Several approaches to spectral analysis have been analyzed theoretically. These include prism and grating spectrometers, interferometers, multislit dispersive systems, and Fresnel zone plate spectrometers. The technique of tunable acousto-optic filtering was investigated experimentally.	4028-1	

CONTENTS

INTRODUCTION	1
RADIOMETRY	1
SPECTRUM ANALYZERS	4
Prism and Grating Spectrometers	6
Interferometers	10
Multislit Dispersive Systems	12
TUNABLE ACOUSTO-OPTIC FILTER (TAOF) IN THE INFRARED REGION	14
Definition of TAOF	14
Design Considerations	15
Experimental Results	17
Future Applications	19
APPENDIX A. A PRISM SPECTROMETER	22
APPENDIX B. SIMPLE ANALYSIS OF A CODED SYSTEM	25

Accession For	
NTIS GRA&I	
DTIC TAB	
Unannounced	
Justification	
By	
Distribution/	
Availability Codes	
Dist	Avail and/or Special
A	

INTRODUCTION

Infrared systems used for a great variety of reconnaissance and surveillance tasks have typically used relatively broad bands of radiation in the 1-3 μm and 8-12 μm regions. Usually the requirements for such systems have been to obtain high spatial resolution over wide fields of view. Of course good sensitivity in the sense of a relatively high signal-to-noise ratio for a small number of photons is desirable.

Additional information is found if the spectrum of the irradiance is obtained instrumentally. Of course one must pay some sort of a price for this additional information. The price usually is fewer photons (or a lower signal-to-noise ratio), a more complex system, and a larger system. The purpose of this report is to provide information about these trade-offs and some of the techniques and instrumental approaches that permit the trade-offs.

The study has been both theoretical and experimental. Several of the relatively modern approaches to spectral analysis have been analyzed and designs have been generated for one or two of these concepts. The technique of acousto-optical filtering was investigated experimentally as well.

RADIOMETRY

The signal-to-noise ratio, SNR, can be obtained from the definition of the detectivity, D^* , of a detector:

$$D^* \equiv \sqrt{A_d B} (\text{SNR}) / \Phi_d$$

where A_d = sensitive area of the detector
 B = effective noise bandwidth
 Φ_d = flux on the detector.

Then

$$\text{SNR} = D^* \Phi_d / \sqrt{A_d B} .$$

If D^* is specified as $D_\lambda^*(\lambda)$ and Φ_d is also a spectral distribution, $\Phi_{d\lambda}$, then

$$\text{SNR} = (A_d B)^{-\frac{1}{2}} \int_{\Delta\lambda} D_\lambda^*(\lambda) \Phi_{d\lambda}(\lambda) d\lambda .$$

If the detector is a typical photodetector with a response that is characteristic of photon response, then

$$D_\lambda^*(\lambda) = D_m^* \lambda / \lambda_m .$$

Thus

$$\text{SNR} = (A_d B)^{-\frac{1}{2}} \left(\frac{hc}{\lambda_m} \right) D_m^* \int_{\Delta\lambda} \Phi_{dq\lambda}(\lambda) d\lambda$$

where h = Planck's constant
 c = speed of light
 λ_m = wavelength of maximum D^*
 D_m^* = D^* at maximum
 $\Phi_{dq\lambda}$ = spectral photon flux at the detector .

There are several different cases that might be considered: the extended source, the subresolution source, a photon-noise limited detector, a current or Johnson-noise limited detector. It is appropriate to rewrite the equation in terms of the source radiation from the target. For an extended target the detector flux can be written

$$\Phi_{dq\lambda} = L_{q\lambda} A_s \Omega_{os} = \tau_o(\lambda) \tau_a(\lambda) A_d \Omega_{od}$$

where $L_{q\lambda}$ = source photon sterance
 A_s = useful area of the source
 Ω_{os} = solid angle subtended at the source by the optics
 Ω_{od} = solid angle subtended at the detector by the optics
 τ_o = transmittance of the optics
 τ_a = transmittance of the atmosphere.

Therefore, for an extended source

$$SNR = (A_d/B)^{\frac{1}{2}} (hc/\lambda_m) D_m^* \Omega_{od} \int_{\Delta\lambda} L_{q\lambda} \tau_a \tau_o d\lambda.$$

For a subresolution source, the detector flux can be written

$$\Phi_{dq\lambda} = I_{q\lambda} \Omega_{os} = (L_{q\lambda} A_s) \Omega_{os}.$$

One does not have knowledge of $L_{q\lambda}$ and A_s generally for a subresolution source. At any rate, it is the product $L_{q\lambda} A_s$ that is measured. Thus

$$SNR = (A_d B)^{-\frac{1}{2}} (hc/\lambda_m) D_m^* \Omega_{od} \int_{\Delta\lambda} I_{q\lambda} \tau_a \tau_o d\lambda.$$

SPECTRUM ANALYZERS

In theory any spectrally dependent phenomenon can be used as the basis of a spectrum analyzer. The most common of these is the spectral dependence of the refractive index. A prism is made; the light is deviated; slits are used; and a spectrometer is born. This is simple and sensitive. However, one could use the principle of internal reflection rather than refraction: scan the prism, always seeking and measuring the critical angle. There seems to be no inherent advantage in this because the critical angle is a sine function as is the simple prism. The technique of focal isolation is a manifestation of chromatic aberration of a lens in the extreme. Thus one can think of a lens as an axial disperser. Of course the angle of reflection is independent of the refractive index, so a reflection spectrometer is not feasible. Brewster's angle depends upon the refractive index which in turn depends upon the wavelength. One could scan an appropriate Brewster plate with auxiliary polarizers, thereby obtaining a measure of the spectrum. The diffraction of light is a wavelength dependent phenomenon, and the classical grating spectrometer makes use of this fact. The ruled grating can be used in transmission or in reflection, and could even be holographic in nature to reduce such things as higher orders of diffraction. Another realization of a diffraction system is the Fresnel zone plate used as a spectrometer. Since the focusing action of the zone plate is wavelength dependent the spectrum will be axial rather than transverse. It can be viewed as a lens with severe chromatic aberration. Other Fresnel diffraction effects could be used. The well known knife edge pattern has peaks in positions dictated by the geometry and the wavelength. This transverse effect could be used with

slits placed properly and the edge scanned. The sensitivity and geometry of this and the other techniques would have to be analyzed before any practical system could be proposed.

Interference phenomena abound; they are all based on a phase difference and in turn the optical path difference (OPD) of two or more beams. The phase difference is $2\pi/\lambda$ times the OPD and the OPD is Δd where n is the refractive index and d is the geometrical path length. Thus the phase shift can result from a change in d or a change in n , or both. In fact

$$\begin{aligned}\Delta\phi &= \Delta(2\pi/\lambda)\text{OPD} \\ &= \phi\left[\frac{\Delta n}{n} + \frac{\Delta d}{d} - \frac{\Delta\lambda}{\lambda}\right].\end{aligned}$$

The most frequent uses of this interference for spectrometers are the Michelson and the Fabry Perot. These have been used extensively and are well described in the literature in many different forms. Other versions of interferometers abound: Lummer Gehrke plates, Smartt, Shearing, Ring, Twyman Green, Fizeau, etc. Some are useful as spectrum analyzers; others are not. The interferometer is, however, a very important kind of spectrum analyzer.

We are left with the phenomena of polarization, scattering and nonlinear effects. The use of a Brewster plate was mentioned above. Other polarizers are based on the orientation of molecules in a material or of wires and are relatively insensitive to wavelength. They can also be based on the anisotropy of refractive index or rotatory effects of crystals. These devolve to the analyses of spectrometers based on dispersion of the refractive index. Polarization can also be generated by scattering, and scattering is dependent

upon the ratio of wavelength to particle size. It is a strong effect when λ/d is small and a relatively mild effect when λ/d is approximately 1. The chief difficulty in using scattering as a wave analyzer is getting the particles to behave and its relative insensitivity.

Nonlinear effects can be considered as interesting ways to generate some of the effects already described. They do have the attributes of flexibility and control that some of the others do not have. Thus they are of considerable interest. One of these is the acousto-optical effect in which a refractive index variation is generated by an acoustic wave. The variation in density makes a sinusoidal grating in the material - and grating analysis applies. A second nonlinear effect is the index variation generated by a high electric field. One then has a tunable filter based on this electro-optical effect. The grating, mentioned above could also be generated by a standing or traveling optical wave. Then one has an opto-optical effect!

These different effects will be treated, with varying emphasis in the rest of this report.

Prism and Grating Spectrometers

In order to avoid all the connotations that arise with the word "spectrometer" the term spectrum analyzer will be used as a generic term describing devices which can be used to measure the spectral components of radiation. The best known of such devices are undoubtedly prism and grating spectrometers. Following Jacquinot, we can write the resolving power and the flux available in a prism or grating instruments as

$$\Phi = \tau L A \cos \theta_i \beta \lambda \frac{d\theta_d}{d\lambda} / Q$$

$$= \tau L \lambda A \cos \theta_i \beta \lambda^2 \frac{d\theta_d}{d\lambda} / Q^2$$

where τ = spectrometer transmission

A = area of disperser

L_λ = spectral radiance

θ_i = angle of incidence on the disperser

β = angular height of the exit slit

$\frac{d\theta_d}{d\lambda}$ = angular dispersion (or diffraction)

Q = quality factor or resolving power

 = $\lambda/\Delta\lambda$.

The normal use of these instruments invokes the use of a single entrance slit and a single exit slit. One is focussed on the other and the disperser (prism or grating) is scanned. Then the exit slit represents one wavelength first, and then another, etc. Such a system requires a relatively high bandwidth. If $\Delta\lambda$ is the total bandwidth and $\delta\lambda$ is the resolution, then N samples must be taken in a time T_s available for the spectrum which is given by

$$N = \Delta\lambda/\delta\lambda .$$

The required bandwidth is given by

$$B = 1/2\tau = N/2T_s = \Delta\lambda/2T_s \delta\lambda .$$

If however, m exit slits are used the bandwidth is decreased:

$$B = N/2mT_s$$

Clearly if the whole spectrum is covered with exit slits, then $m = N$ and $B = 1/2T_s$. This illustrates the fact that the multiplex advantage applies to these devices when multiple slits are used. Some care must be taken to the way this is applied to a particular realization.

Questions to be asked about these techniques are how wide a field of view can be accommodated for the given time T_s , spectral interval $\delta\lambda$, and spatial interval $\Delta\theta$.

For these two types of spectrometers, the available flux and the square of the resolving power are inversely related. Further, for a detector that obeys the square-root-of-area law one has

$$D^* = \frac{\sqrt{A_d}}{\Phi_d} \text{ SNR}$$

$$\text{SNR} = \frac{D^* \Phi_d}{\sqrt{A_d} B} .$$

Thus $\text{SNR} = \frac{D^* \tau L \lambda A \cos \theta_i \beta \lambda^2}{Q^2 \sqrt{A_d} B} \frac{d\theta_d}{d\lambda} .$

The area of the detector is independent of the other parameters only if recollecting optics are used. If the detector becomes the exit slit, then it must have angular dimensions given by

$$\frac{\beta \lambda^2}{Q} \frac{d\theta_d}{d\lambda} .$$

Therefore

$$\text{SNR} = \frac{D^* \tau L_\lambda A \cos \theta_i \beta^{\frac{1}{2}} \lambda}{QB^{\frac{1}{2}}} \left(\frac{d\theta_d}{d\lambda} \right)^{\frac{1}{2}}.$$

Then for a multiple-exit-slit instrument

$$\frac{\text{SNR}}{L_\lambda} = \frac{D^* \tau A \cos \theta_i}{Q} \left(\frac{\beta 2mT_s d\theta_d}{Nd\lambda} \right)^{\frac{1}{2}}.$$

From this we can see that the linear factors affecting the SNR are D^* , transmission, size of the dispersing element, and the resolving power. The square-root terms include the exit slit height, number of detectors, dispersion, and number of spectral elements. A comparison between the prism and the grating need be done only on the basis of $d\theta_d/d\lambda$.

The field of view characteristics of these two instruments can be considered separately for the two different directions, in the direction of dispersion and orthogonal to it. Different portions of the source will be imaged at different vertical positions of the slit. Thus, if each slit is made up of a vertical array of detectors each detector will sense the quasimonochromatic radiation from a different part of the (vertical) field. The width of the slit and the dispersion of the grating or prism determine the spectral purity or spectral slit width. These factors also determine the separation between exit slits in a multiple-slit spectrometer. Accordingly, to obtain the spectrum of the elements of a scene, one can disperse in one direction using narrow-field optics but image a wide field in the other direction. A design example is considered in Appendix A.

Interferometers

The Michelson and Fabry Perot interferometers have been used as spectrum analyzers. They both enjoy the multiplex advantage because they view every spectral element for the time T_s . Both have a throughput that is higher than slit spectrometers. In fact the flux is given by

$$\Phi = L_v (\pi r^2 / f^2) A \tau \Delta v$$

$$\Phi = L_v 2\pi A \tau v / Q^2$$

$$\frac{SNR}{L_v} = \frac{2\pi A \tau v D^*}{(A_d B)^{1/2} Q^2}$$

where A = interferometer plate area

τ = transmission

B = bandwidth

A_d = detector area .

The bandwidth in this case is $1/2T_s$ because every wavelength is viewed all the time, $N = m$. The detector area will be determined by the properties of the "camera lens." One could take a ring of the interference pattern and focus it to a detector, or he could just use the size of the central maximum.

For simplicity we take the latter and assume the detector is also circular. Then

$$\frac{SNR}{L_\lambda} = (2\pi T_s)^{1/2} A \tau v D^* / r Q^2 .$$

We have the SNR per unit spectral radiance as a function of system parameter. In addition to the questions of resolving power and throughput, one should also be concerned about the instrumental profile and response to transients.

It seems obvious that any scanning instrument, whether it be an interferometer or slit spectrometer, suffers from the fact that a transient cannot be differentiated from characteristics in the spectrum without an auxiliary measurement. For an instrument that scans the spectrum (rather than the interferogram) a monitor that senses all the spectrum can be used. Then the output is calculated as $\phi_{d\lambda}/\phi_d$ at all times. The result is direct and accurate. A Fourier transform spectrometer, however, takes some additional thought. We assume that a spectrum $F(\omega)$ is to be obtained from an interferogram $f(t)$. During the scan, say half way through, the total intensity is changed by an amount $f_1(t-t_0)$. From the additive property of transforms the output spectrum will then be

$$F(\omega) + F_1(\omega-\omega_0).$$

The spectrum will be the combination of the spectral distribution of the source and the spectrum of the perceived fluctuation of the total intensity of the source. One solution to this problem is the measurement of this second quantity and appropriate processing. A second and more insidious problem is one that results from the modulation of individual components of the radiation. This could happen for instance in a source in which there was mode hopping. The analysis of such a situation is left for later study.

Multislit Dispersive Systems

The simplest multislit system is one in which a single entrance slit is used and a detector is used in every position where a spectral line is to be measured. If the detectors are just placed side by side and as closely packed as possible, this can be viewed as a simple spectrometer. One could also place the detectors strategically with respect to spectral lines and get a correlation spectrometer (correlating an unknown signal with the assumed spectrum). An alternative is to use a strategic array of slits and focus all the output on a single detector - still a correlation spectrometer. These devices have the multiplex advantage, but not the throughput advantage. In the so-called Haddamard system, a single detector senses the radiation from a coded array of slits. Golay and Felgett have described the use of such slit arrays, which are binary and orthogonal and Decker has described the type of spectrum analysis generally called Haddamard transform spectroscopy (HTS). One can use both multiple entrance slits and multiple exit slits and obtain the spectrum of every resolution element in the scene, an imaging spectrometer.

Decker has described an HTS for spacecraft use. We follow his description here. The ratio of SNR's for an HTS to a single slit dispersive spectrometer is

$$\frac{1}{2} (nN)^{\frac{1}{2}}$$

where n is the number of entrance slits and N the number of exit slits.

For a multiple exit slit spectrometer the gain would only be $\frac{1}{2} \sqrt{n}$.

This amounts to the throughput gain alone. But the other dimension of the coded mask can be used for spatial scanning. A system with 1023 spatial elements and 63 spectral elements was flown by NASA. It scanned the spectrum from 2 to 25 μm in 2 sec.

Fresnel Zone Plate Spectrometer (FZPS)

It is well known that a Fresnel zone plate can be used like a lens. The light is blocked from alternate half-period zones, each with arc length measure of the width of each zone s_m and the focal length is then given by

$$f = \frac{s_m^2}{m\lambda} = \frac{s_1^2}{\lambda}$$

where

s_1 = measure of the first zone width.

There are secondary foci at $f/3$, $f/5$, $f/7$, ... the origin of which can be understood from an analysis of half-period zones. As illustrated in Fig. 1, the axial distance from a spherical wave to a point P is called b. Then the height along the spherical wave is such that $b_1 = b + \lambda/2$, $b_2 = b + 2\lambda/2$, etc. To first order, all the odd rings add in phase at P and all the even rings add in phase together but out of phase with the odd rings. Thus if the one alternate set of rings is eliminated, the other set contributes

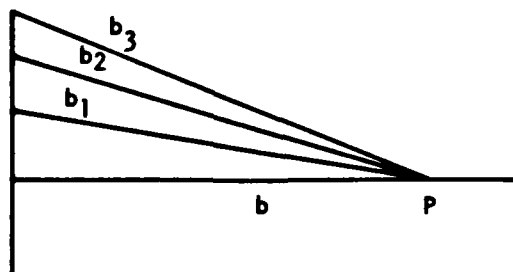


Fig. 1. Axial distance from spherical wave to point P.

waves that add in phase. Now consider a point P' at some position closer to the wavefront. The math is tedious and just shows that there are these secondary focal points closer to the zone plate.

If this device is to be used as a spectrometer, then polychromatic light will shine on it and be focused at s_1^2/λ_1 , s_1^2/λ_2 , ... The axis separations Δb are $s_1^2(\frac{1}{\lambda_1} - \frac{1}{\lambda_2}) = \frac{s_1^2}{\lambda^2} \Delta\lambda$. For example, if s_1 is 1 cm and λ is 1 μm , then $\Delta b = 10^8 \Delta\lambda$; a spectral separation of 0.1 μm results in an axial separation of 10 m! But if λ is 10 μm , then the separation is 10 cm. In practice one would use a smaller value for s_1 . The longer wavelengths of light will be focused closer to the zone plate, since the focal length is inversely proportional to the wavelength. The detectors or mirrors can be placed axially, thereby generating a certain amount of obscuration to successively shorter wavelengths.

TUNABLE ACOUSTO-OPTIC FILTER (TAOF) IN THE INFRARED REGION

Definition of TAOF

The tunable acousto-optic filter (TAOF) is an electronically tuned optical filter that operates on the principle of acousto-optic diffraction. The spectral passband of the filter can be rapidly tuned over wide spectral regions by simply changing the frequency of the applied RF signal.

Most of the TAOF's reported have been operated in the visible and ultra-violet spectral regions. Extension of the TAOF spectral range into the infrared is more difficult due to the lack of efficient infrared TAOF materials. The TAOF's developed thus far have used $\text{Tl}_3\text{AsSe}_3^{(1)}$ and TeO_2 as the filter material.

We have developed and will describe an IR TAOF using LiNbO_3 .

Design Considerations

The first TAOF⁽²⁾ was made by Harris et al. using LiNbO₃ as TAOF material. It has an optical frequency given by

$$f_o = \frac{c}{v} \frac{1}{|\Delta n|} f_a$$

f_a = RF acoustic frequency

c/v = velocity of light $\frac{\text{in vacuum}}{\text{in medium}}$

Δn = birefringence of the material.

The tunable optical wavelength of this TAOF was restricted to the visible region. It was operated by a CdS thin film transducer and was centered at about 864 MHz (corresponding to 6328 Å).

This kind of filter can have its tunable optical wavelength in the IR region, if a transducer whose center wavelength lies in the infrared region can be made. In the filter configuration described in Fig. 2, linearly polarized infrared light is normally incident through a silicon wafer on a 2-inch long crystal of 90° cut LiNbO₃. It propagates collinearly with a longitudinal acoustic standing wave along the x axis of the crystal. The incident light may be polarized along either the y or z axes. Diffraction into the orthogonal polarization is only cumulative if $|k_o| - |k_e| = |k_a|$, where the subscripts o, e, and a denote the ordinary, extraordinary optical waves, and the acoustic wave respectively. This has been already expressed as $f_o = c f_a / v |\Delta n|$. For LiNbO₃ $v \approx 6.57 \times 10^5$ and $\Delta n \approx 0.08^*$; and thus $f_o \approx 5.7(10^5) f_a$. The tuning curve of this filter is shown in Fig. 3.

* $\Delta n = 0.08$ at 3.39 μm, $\Delta n \approx 0.09$ at visible region

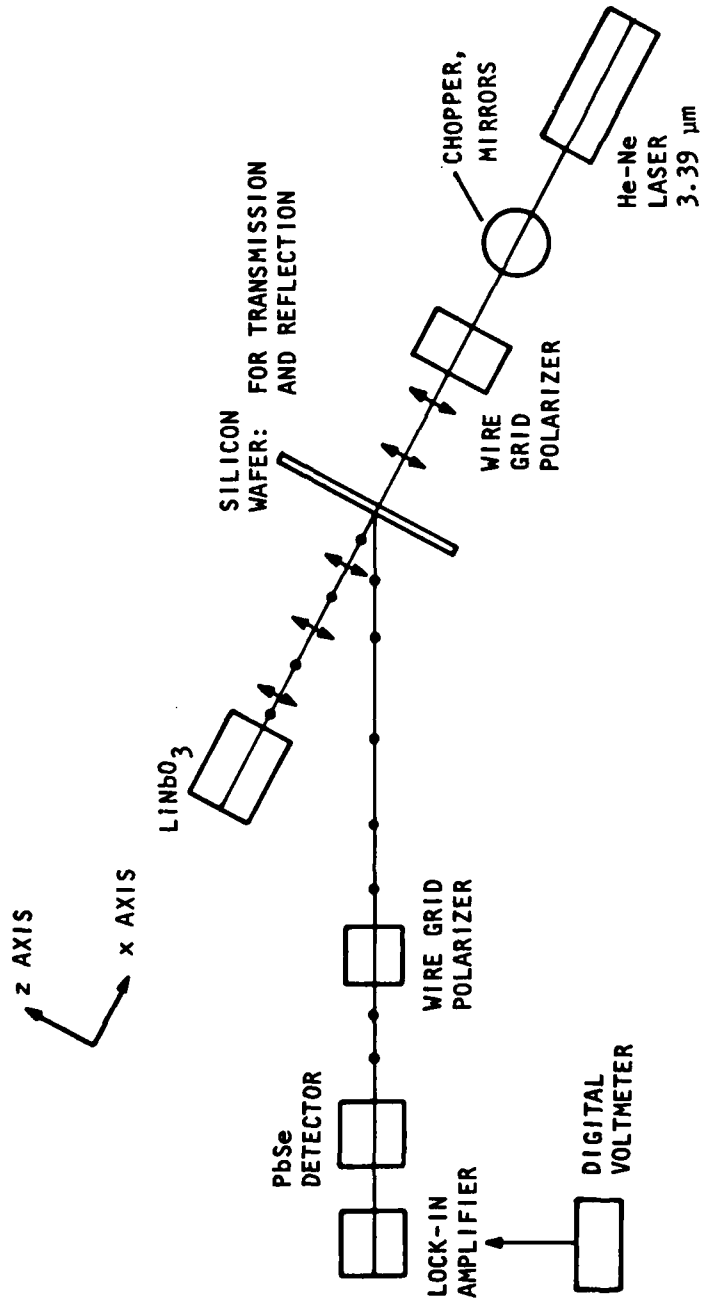


Fig. 2. Experimental setup for an IR TAOF using LiNbO₃.

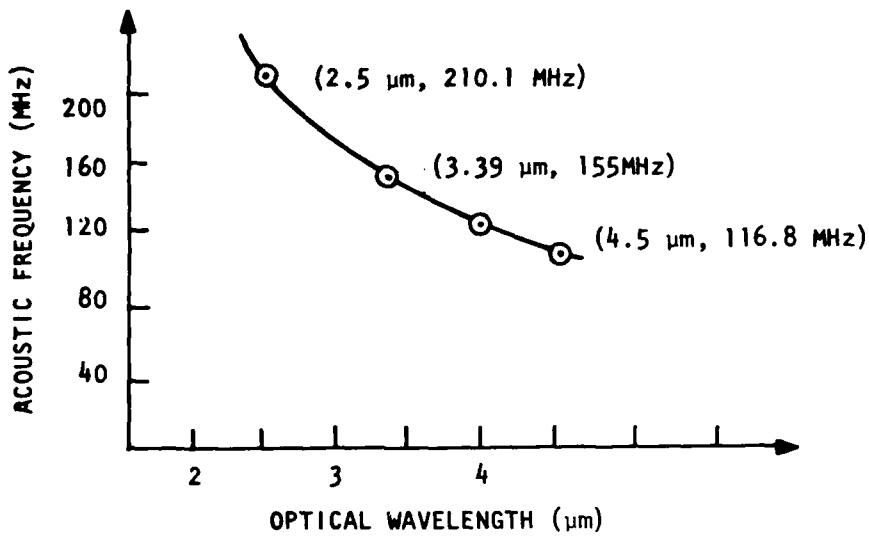


Fig. 3. Theoretical tuning curve for an IR LiNbO_3 TAOF (in collinear mode).

Experimental verification of the tuning curve has been achieved at the wavelength of $3.39 \mu\text{m}$ of a HeNe laser. The acoustic frequency calculated by the equation $f_o = cf_a/v|\Delta n|$ was 150.0 MHz. This frequency is in good agreement with the measured value of 154 MHz.

Experimental Results

A LiNbO_3 crystal 2-inch x 1/2-inch x 1/2-inch (x, y, z axis) made by Crystal Technology Inc. was used. The LiNbO_3 crystal was polished flat and parallel in order to enhance the longitudinal acoustic resonances. One side of this crystal was gold vacuum deposited to operate the filter in the reflection mode. After the vacuum deposit, a 36° rotated y-cut transducer

was attached using Lens Bond and its thickness was reduced to about 36 μm .

Another gold deposit of 5.0 mm^2 was made for the top electrode of this transducer.

To cross check the filter performance, light deflection and modulation by acoustic energy was tested experimentally. The Bragg deflection formula was confirmed. In Fig. 4 light is diffracted due to the longitudinal acoustic wave through the medium.

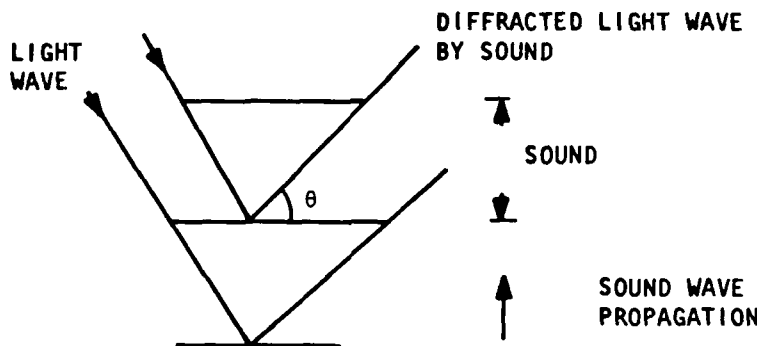


Fig. 4. Acousto-optic light deflection in LiNbO_3 .

The angle θ is related to other parameters by the following equation

$$2\lambda_s \sin\theta_L = \frac{\lambda_0}{n}$$

λ_0 = optical wavelength

λ_s = velocity of sound in LiNbO_3
acoustic wave frequency

θ_{air} = $n_L \times \theta_L$

n_L = LiNbO_3 index of refraction

θ_L = angle in LiNbO_3 .

The measured angle of 4.28 mr was in good agreement with the value of 4.20 mr. The experimental results of the operation of this TAOF were obtained using a lead selenide detector and lock-in amplifier (Princeton Applied Research HR-8). The minimum noise level was \pm 0.2 mV. The resolution over 3.39 μm peak was calculated by the experimental curve. In Fig. 5 the half bandwidth frequency is 154.8 MHz (3.40 μm). The difference between this value and 3.39 μm is 8.7 cm^{-1} . In case (1) of the figure the filter has a smaller bandwidth than that of case (2). The power density was approximately $40 \frac{\text{mW}}{\text{mm}^2}$ in case (1) and $30 \frac{\text{mW}}{\text{mm}^2}$ in case (2). At the peak of the passband, transmitted optical intensity of case (1) is larger than that of (2) due to the larger power density in the transducer. The transmitted light intensity is related to the expression

$$\sin^2 \pi \sqrt{\frac{L^2 \lambda^2}{2 \mu_2} \cdot (\text{power density})^{-1}}$$

In this case the half bandwidth can be reduced to 1 cm^{-1} by increasing the power density in the transducer. This has not been tried because we did not want to overdrive the amplifier.

The measured center peak of transmission 1540 MHz was in good agreement with the 155.0 MHz calculated. The error was within 1% and it could be due to the error of the frequency measurement itself.

Future Applications

With a tunable collinear CaMoO_4 filter inside the cavity of the dye laser, electronic control of the laser output wavelength was achieved over a range of 0.5445 μm to 0.6225 μm by D. J. Taylor et al.⁽³⁾

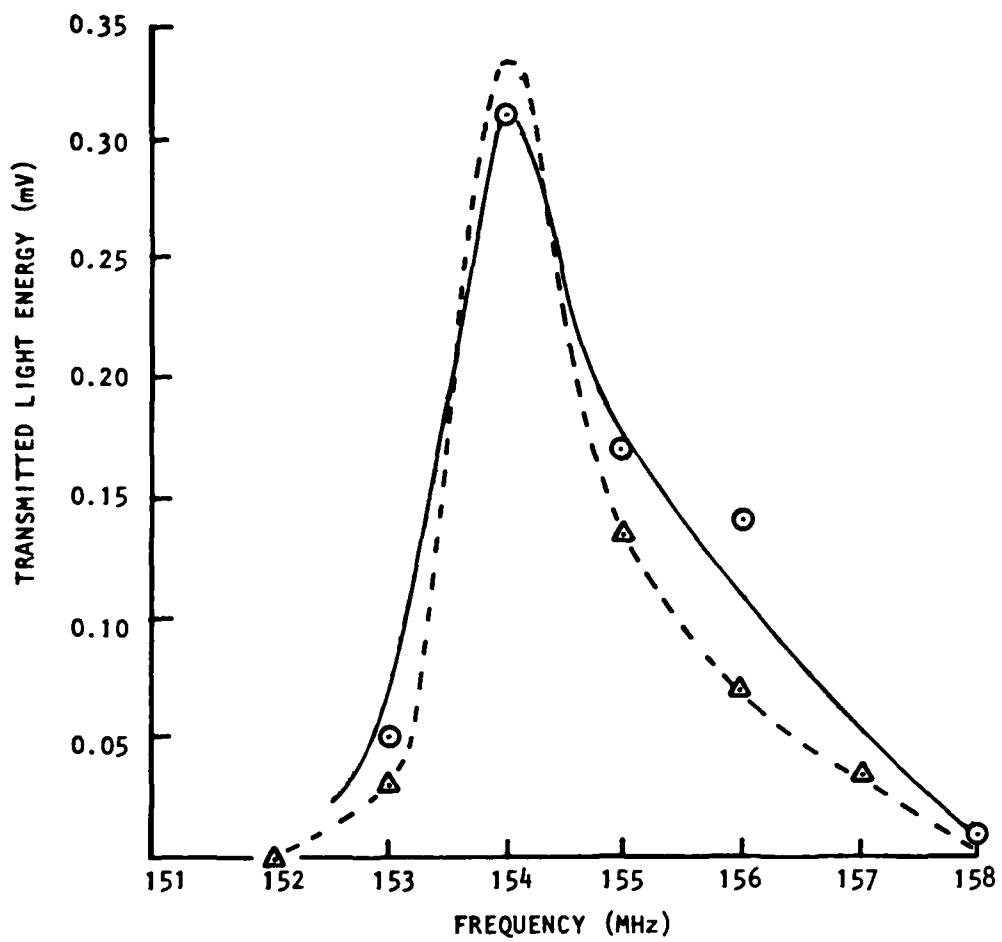


Fig. 5. Frequency spectrum of $3.39 \mu\text{m}$ He-Ne laser by TAOF scanning. (---) First scanning, 40 mW/mm^2 . (—) Second scanning, 30 mW/mm^2 .

In the infrared region near 10 μm , there are two problems in obtaining this type of laser-output control. One is the crystal itself. Almost all oxides exhibit strong lattice absorptions beginning at about 4.5 μm and are thus no longer suitable at 10 μm region. There are many crystals under study⁽⁴⁾ and many have satisfactory transmission and acousto-optical coefficients (see Table 1 for six of them). They are too small, however.

Table 1. Infrared TAOF Materials.

Material	Space Group	Transmission in μm	n	Δn	$M_f \left(\frac{10^{-15}}{5^3/\text{g}} \right)$	Interaction Geometry
CdGeP ₂	42 m	0.72-13	3.31	0.01	-	Noncollinear
AgGaSe ₂	42 m	0.73-18	2.62	0.032	-	"
CdSe	6 m	0.75-25	2.45	0.02	-	"
AgAsS ₃	3 m	0.6-14	2.86	0.19	-	Collinear or noncollinear
Tl ₃ AsSe ₃	3 m	1.21-14	3.34	0.187	0.67	"
Te	32 m	4-25	6.25	1-45	-	"

Another problem is to get efficient birefringent polarizing elements if the filter is to be operated in the reflection mode at longer wavelength. This problem can be solved if simple geometry is used instead of sophisticated beam splitting process in the reflection mode. Chang's⁽⁵⁾ "walk off" type can be one example.

APPENDIX A

A PRISM SPECTROMETER

The design of a prism spectrometer for wide fields of view requires the design of fore optics and prism optics. Let us assume that the field of view required is 1° , the resolution $100 \mu\text{rad}$ and the resolving power $100 - 1000$ for the intermediate infrared, $3-5 \mu\text{m}$.

We will start at the back, the monochromator design. Most of the equations we need are given by Sawyer. The resolving power Q is given by

$$Q = \Delta t \frac{dn}{d\lambda} = \frac{2a \sin\alpha/2}{\cos i} \frac{dn}{d\lambda}$$

where Δt = the difference in prism thickness at the two ends

a = prism area

α = prism angle.

The dispersion is given by

$$\Delta x = f\Delta\theta = f\Delta n 2\sin\alpha / \sqrt{1-\bar{n}^2 \sin^2\alpha/2}$$

where Δx = linear dispersion (separation of λ 's)

f = focal length

$\Delta\theta$ = angular dispersion

\bar{n} = average refractive index.

We need to make some other choices. These include the size of the prism (really the beam) and the speed of the optics. Take these as 20 cm and F/2.5. This means that the focal length is 50 cm. Therefore a detector

which subtends 100 μ rad must have a linear dimension of 50 μ m. This is a convenient size. Also then $\Delta\theta = 100 \mu$ rad. Therefore

$$\frac{\sin\alpha}{\sqrt{1-\bar{n}^2\sin^2\alpha/2}} = \frac{\Delta\theta}{\Delta n} .$$

If we choose germanium as a first trial material, then the refractive index values at 3 μ m and 5 μ m are

$$\bar{n} = 4.0471$$

$$\Delta n = -0.0651 .$$

A solution by trial and error then gives

$$\alpha = 1.757^\circ.$$

This is a remarkably small angle, but germanium has a very large index. At this point in the design we have a choice of the kind of mount to use. The simplest is just a prism with the light passing through to a second lens or mirror. One can also use a Littrow mount in which a mirror is placed behind the mirror. This way one obtains a double pass of the prism for added dispersion. Another alternative is to silver the back face of the prism in which case only a singlepass amount of dispersion is obtained because the back face interaction is a single reflection and not a refraction.

We have calculated that a prism angle of 1.757° is appropriate for the angular dispersion and resolving power of the problem. If we use the

calculate) the deviation is given by (for a nominal index of 4.9):

$$\begin{aligned}\delta &= \sin^{-1}(n \sin(\frac{1}{2}\alpha)) - \alpha \\ &= 1.759\end{aligned}$$

The deviation will be divided equally by the front and back surfaces. If the prism is silvered on the back the front surface will do all the dispersing but it will be divided equally between the forward pass and the backward pass. The same dispersion will be generated. In the Littrow, a separate mirror is used and the central ray retraces itself to the prism where it is refracted at both surfaces and sent back along an angle of about 3.52° with respect to its direction of incidence (and reversed).

Now all of this happens in the direction of dispersion, in the direction of the entrance slit width. The field of view is in the direction of the slit height. For this problem we have specified a full field of 1° and a resolution of $100 \mu\text{rad}$. The third order equations tell us that spherical aberration must be corrected, that coma is about $87.5 \mu\text{rad}$ for an F/2.5 system and that astigmatism is about $15 \mu\text{rad}$. Added together they nearly meet the specification, but to obtain some design margin we should consider a Ritchey Chretien and thereby obtain zero spherical and comatic aberration. The diffraction blur circle (Airy disc) will be $2.44 F\lambda$ or $30.5 \mu\text{m}$ at $5 \mu\text{m}$. This is smaller than the detector we chose and therefore all right.

The rest of the design has to do with layout, obscuration, spectral purity, etc. They will not be considered here.

APPENDIX B

SIMPLE ANALYSIS OF A CODED SYSTEM

Imagine a linear three-element field of view, the elements are labelled 1, 2, and 3. If a mask that has an opening in the first two positions but is closed in the third, covers this field, then the detector viewing this sees a signal v_a given by

$$v_a = \ell_1 + \ell_2$$

where ℓ_i = radiance as modified by responsivity, transmission, etc.

If at the next instant a mask with elements 2 and 3 open is put in place, then

$$v_b = \ell_2 + \ell_3.$$

Finally $v_c = \ell_1 + \ell_3.$

The last is for a mask with 1 and 3 open. These are three independent equations in three unknowns. The radiances can be found

$$\ell_1 = \frac{1}{2} (v_a - v_b - v_c)$$

$$\ell_2 = \frac{1}{2} (-v_a + v_b - v_c)$$

$$\ell_3 = \frac{1}{2} (-v_a - v_b + v_c).$$

This is an appropriate system for three-element spatial scanning. We can imagine however that a disperser has spread the spectrum across these elements so that the ℓ 's can be thought of as wavelengths. Then a spectral

scan results. It is easy to imagine how one can scan both spatially and spectrally if the scanning were indeed done in both directions. It is harder to see how a two-dimensional situation works. The linear code is illustrated by the following horizontal (row) vector where 1's mean transmission and 0's mean blockage:

110110110110.

We can imagine a window that moves along this mask, taking three elements at a time:

110
101
011
110
.
.
.

It is cyclic with a period of three. Each group of three gives a set of independent equations which can be solved as above. Now we will establish a second row below the first:

110110110
101101101 .

It is an identical row, but it has been moved one element to the left. Both rows clearly provide the necessary spectral information. We can repeat the procedure with another row

011011011
110110110
101101101
011011011
110110110.

Now we can look at successive 3x3 array inputs (all of which will be seen by the detector):

$$\begin{aligned}v_a &= l_{11} + l_{12} + l_{21} + l_{23} + l_{32} + l_{33} \\v_b &= l_{12} + l_{13} + l_{21} + l_{22} + l_{32} + l_{33} \\v_c &= l_{11} + l_{13} + l_{22} + l_{23} + l_{31} + l_{32} \\v_d &= l_{11} + l_{12} + l_{21} + l_{23} + l_{32} + l_{33}.\end{aligned}$$

Since v_d is equal to v_a there is no new information. Further it can be seen that any three-position movement places the original nine-element array over one that is identical. In order to decode this we need another array which combines with this one. If an identical array is used, similar results are obtained. Decker shows that there are masks that can be used, but that no simple rule exists for finding them. It is clear that from what we have done above, a larger mask is in order. Consider the problem of scanning three spectral intervals and two spatial positions. There are six independent unknowns. Suppose, although it is not the best code, we choose

11110001111000
11100011110001.

The individual output readings as a 3x2 window slides over this one

$$\begin{aligned}v_a &= l_{11} + l_{12} + l_{13} + l_{21} + l_{22} + l_{23} \\v_b &= l_{11} + l_{12} + l_{13} + l_{21} + l_{22} \\v_c &= l_{11} + l_{12} + l_{21} \\v_d &= l_{11} \\v_e &= l_{23} \\v_f &= l_{13} + l_{22} + l_{23}.\end{aligned}$$

From these we find immediately that

$$\ell_{23} = v_c, \ell_{11} = v_d, \ell_{23} = v_a - v_b.$$

But further investigation shows that $v_a = v_c + v_f$. These are not linearly independent equations. They will not provide a solution. We picked the code incorrectly. The fact that codes can be chosen to accomplish the task has been demonstrated both theoretically and experimentally. The problems which remain are the nasty engineering ones of obtaining high resolution over wide fields with good out-of-band rejection and excellent spectral profile.

REFERENCES

1. Feichtner, J. D., M. Gottlieb, and J. J. Conroy, "A tunable collinear acousto-optic filter for the intermediate infrared using single crystal Tl_3AsSe_3 ," SPIE Vol. 82, Unconventional Spectroscopy, p. 106 (1976).
2. Harris, S. E., S. T. K. Nieh, and K. D. Winslow, "Electronically tunable acousto-optic filter," Appl. Phys. Lett. 15, 325 (1969).
3. Taylor, D. J., et al., "Electronic tuning of a dye laser using TAOF," Appl. Phys. Lett. 19, 269 (1971).
4. Katzka, P. and I. C. Chang, "Acousto-optical properties of chalpyrite compounds," IEEE Proc. 1977 Ultrasonics Symposium, p. 436.
5. Chang, I. C., "Tunable acousto-optic filter utilizing acoustic beam walk-off in crystal quartz," Appl. Phys. Lett. 25, 323 (1974).

DAT
FILM